Chapter 4

Retinal blood vessels segmentation by using Gumbel probability distribution function based matched filter

4.1 Introduction

The retinal blood vessel's structure contains the important information which is helpful for the detection and diagnosis of various retinal pathology such as hypertension [139], glaucoma [140],diabetes [26],[66],[27] etc. The ophthalmologist scans the retina of the patients by using high resolution fundus camera and then prob the situation of retinal blood vessels to diagnose the retinal diseases [13]. In some cases it is found that the retinal blood vessels have low contrast with respect to their background. and it becomes difficult to diagnose the retinal disease. Therefore, it is necessary to apply suitable image segmentation technique for accurate detection of retinal blood vessels. These techniques are based on the image features such as the cross-sectional profiles, uniform intensity regions and edges. The intensity of the retinal blood vessel changes smoothly, so normal edge based models such as gradient based operators [149],[150],[151], Robert's and Krisch differential operators [152], Prewitt operators [153], Sobel operators [154] are not suitable to identify them accurately.

The author Fraz *et al.* [6] classify the retinal blood vessel segmentation approaches into seven categories on the basis of retinal image features, namely, the intensity based pattern recognition techniques [27, 30, 53, 50], mathematical morphology based [2], [155], [156], vessel tracking based [69], model based [34, 35, 157], parallel hardware based [41, 42], multi-scale based techniques [158, 159] and matched filter based techniques. [12, 2, 13, 47].

4.2 Background

The proposed Gumbel probability distribution function based retinal image segmentation approach comes in the category of matched filter based approach. In this section, our objective is to present,how much work has been done previously. The matched filter based retinal blood vessel segmentation approach provides the best retinal vessel structure with respect to other filtering approaches [12],[2],[13],[47]. The matched filter based approaches compare the variations of the intensity level of the cross-section profile of the retinal image with the predetermined template or kernel. The first matched filter based retinal blood vessel segmentation approach was proposed by Chaudhuri *et al.* [12]. The matched filter based approach detects the retinal blood vessel by applying the matched filter kernel and thresholding on the original input retinal image [12]. To design a matched filter kernel, three points are important which include limited curvature of vessels which may be approximated by bell-shape piecewise linear segments and the width of the vessels gradually decreases when one move away from the optical disk of the retinal image, and cross-sectional intensity profile of retinal blood vessels. Chaudhuri *et al.*[12] stated that the cross-sectional profile of retinal blood vessels has an approximate Gaussian shape. Hence the Gaussian shaped matched filter kernel is reported in literature for the detection of retinal blood vessels.

According to the literature survey on matched filter based approach, it was found that the many authors improved the performance of matched filter based approach by improving the thresholding techniques [138, 44] rather than changing the Gaussian shaped matched filter kernel. The matched filter based approaches use the prior knowledge about

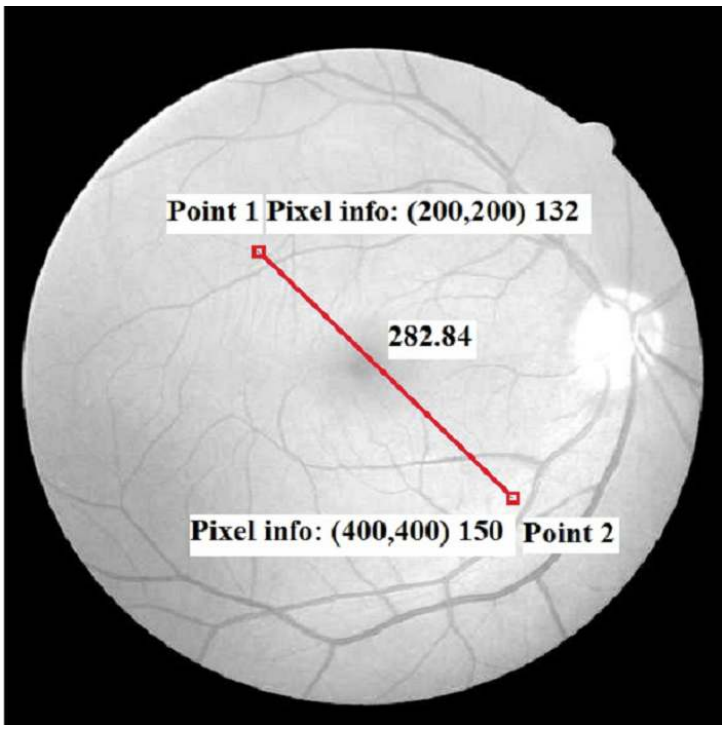

(a)

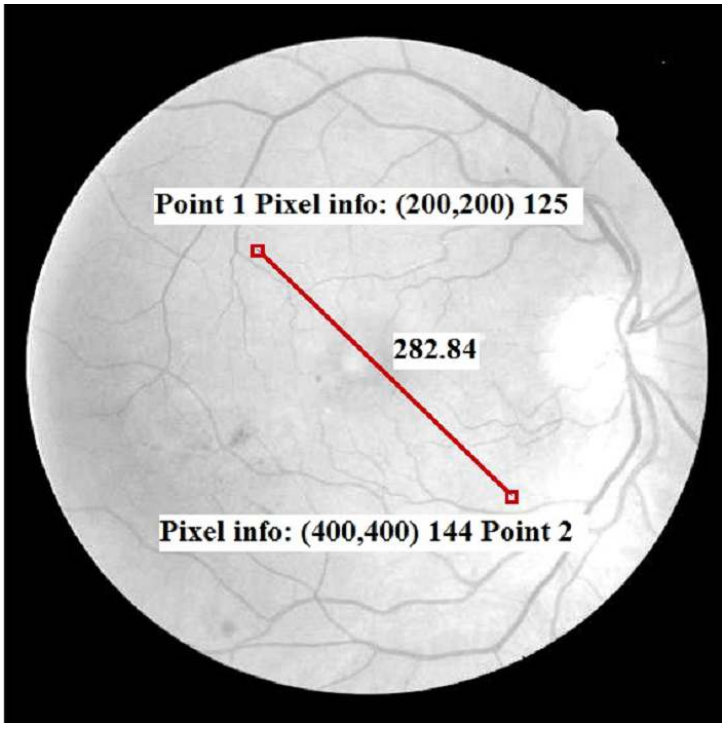

(b)

Figure 4.1: (a) Gray scale retina image of '13_test.tif', (b) Gray scale retina image of '14_test.tif'

the shape and symmetry of the cross-section profile of the retinal blood vessel with respect to their location and scale parameter. Therefore, author H. Zolfagharnasa *et al.* [14] replaced the Gaussian function based matched filter by Cauchy probability density function

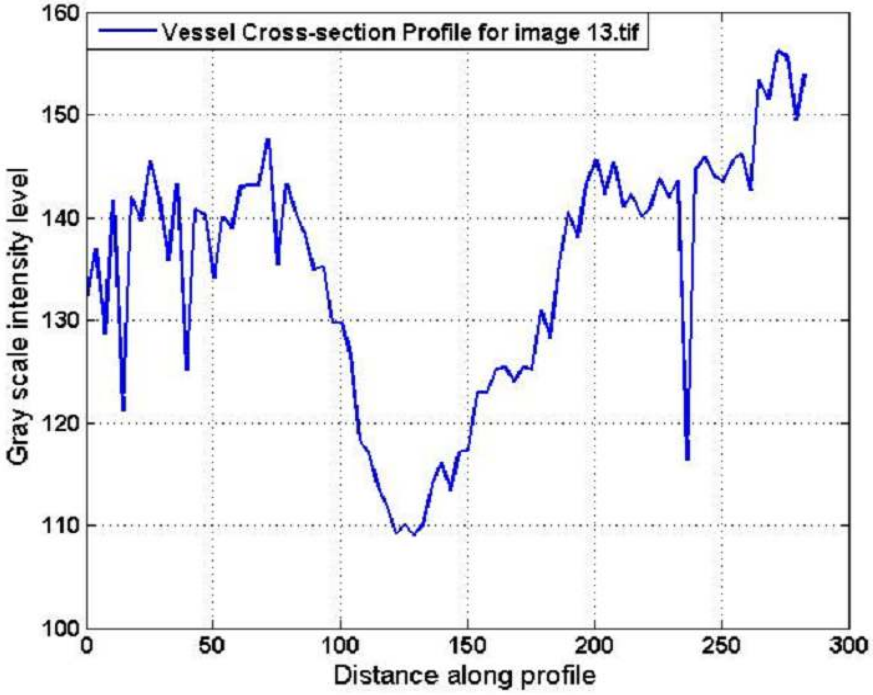

(a)

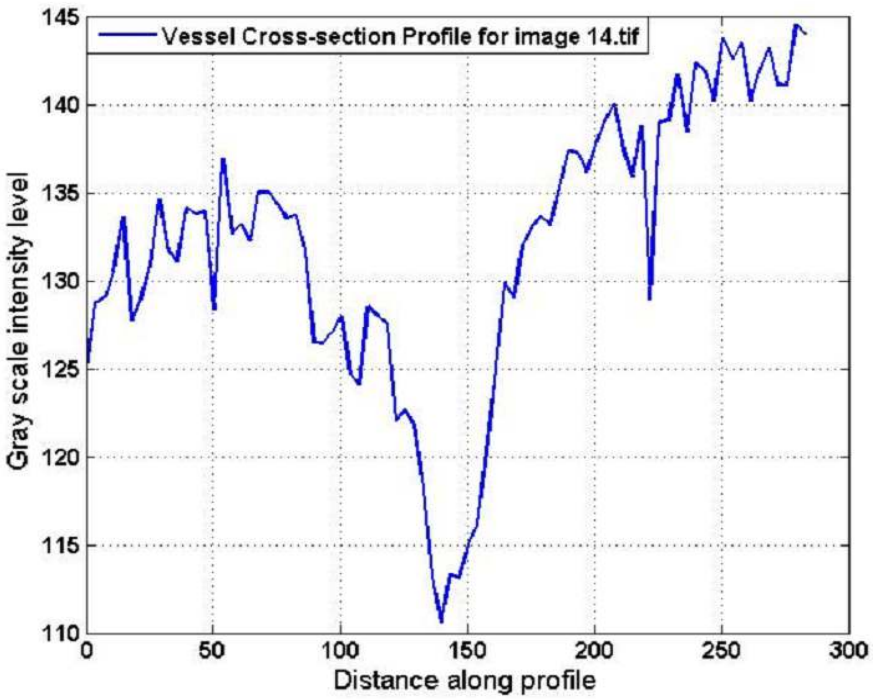

(b)

Figure 4.2: Cross-section intensity profile of the region marked in Figure 4.1(a) and (b) by selecting 80 pixels between two points are presented in (a) and (b) respectively

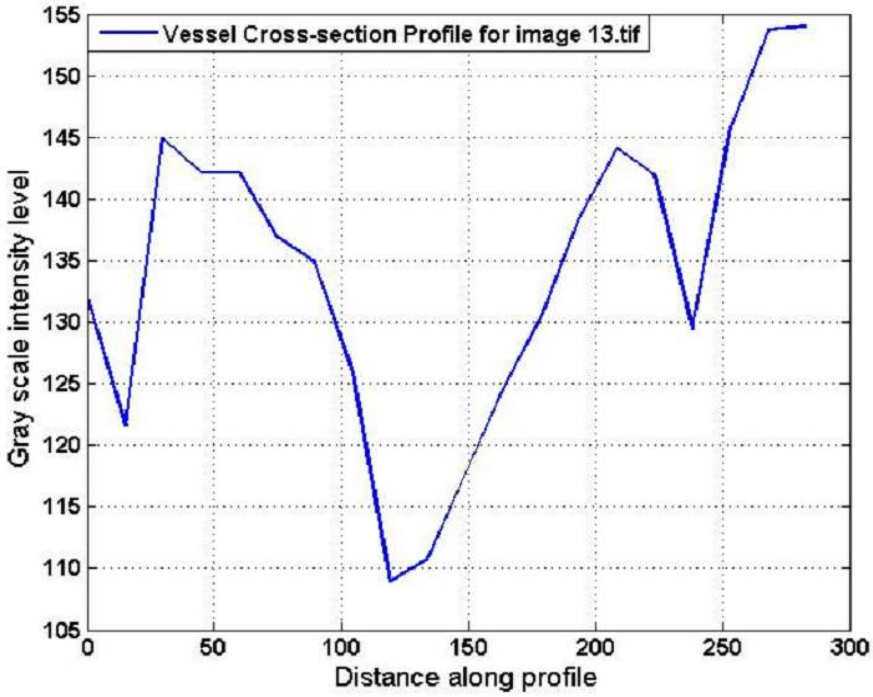

(a)

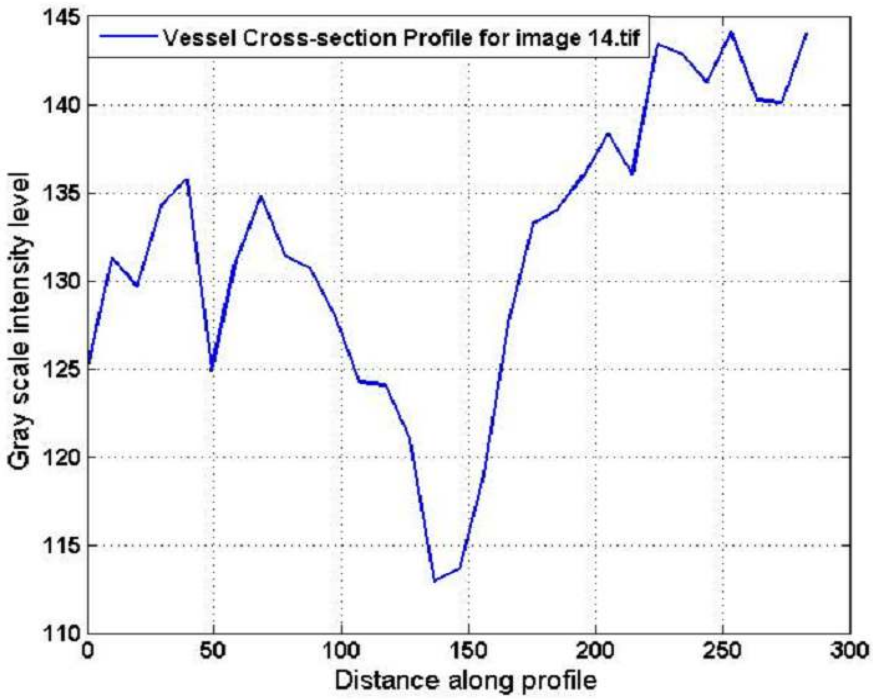

(b)

Figure 4.3: Approximate well shaped cross-section intensity profile of the region marked in Figure 4.1(a) and (b) by selecting 30 pixels between two points are presented in (a) and (b) respectively.

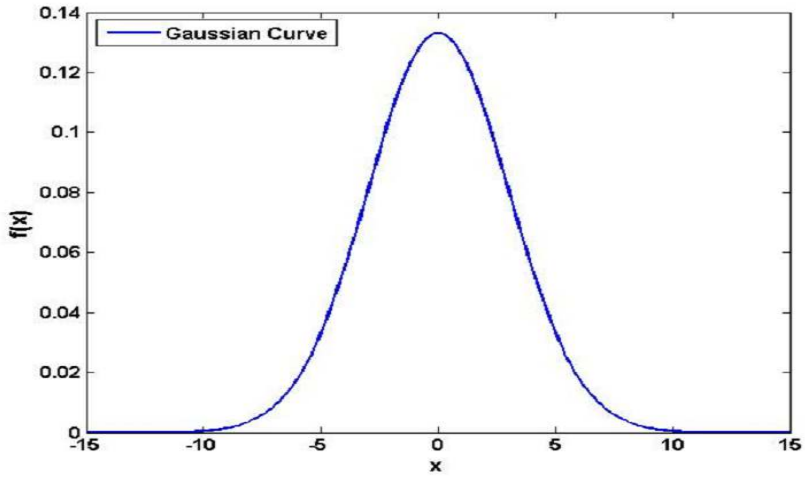

(a)

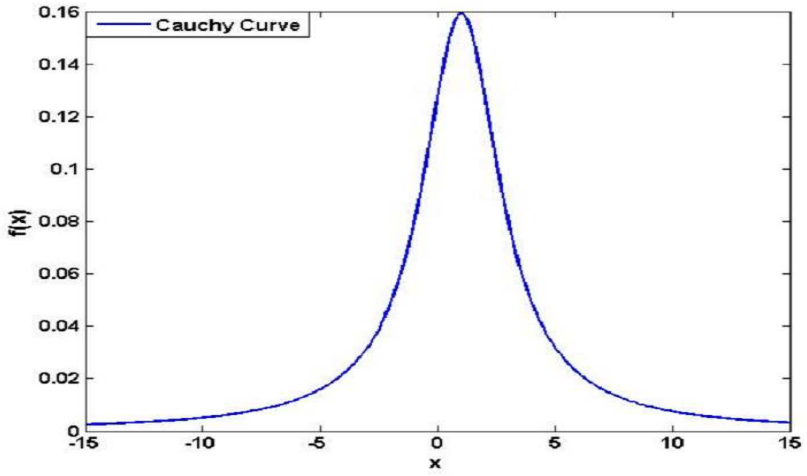

(b)

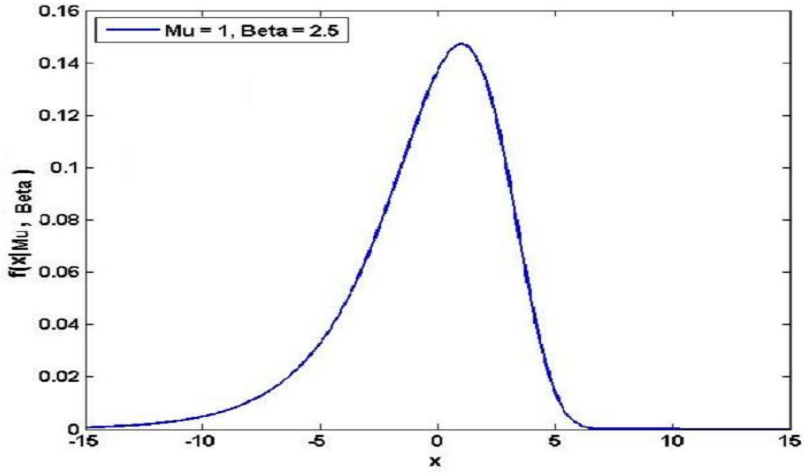

(c)

Figure 4.4: (a) Gaussian distribution Curve, (b) Cauchy pdf Curve, (c) Gumbel pdf Curve

(pdf) and reported that the accuracy of retinal blood vessel detection was substantially improved.

If we visually compare the cross-section intensity profile of the region marked in Figure 4.1(a) and Figure 4.1(b) by selecting 80 pixels between two points, as shown in Figure 4.2(a) and Figure 4.2(b), or their approximate well shaped cross-section profile by selecting less number of pixels (30 pixels) between the selected points, as shown in Figure 4.3(a) and Figure 4.3(b), with the actual Gaussian, Cauchy, and Gumbel pdfs curves as shown in Figure 4.4(a), (b), and (c), it is observed that the Gumbel pdf provides better match with the cross section profile in comparison to Gaussian and Cauchy pdf curves because the Gumbel pdf curve is slightly skewed with respect to the Gaussian and Cauchy pdf curves.

After that in this approach we analyze the gray scale cross-section profile data of retinal image statistically and found that cross-section profile of all 20 retinal images (selected from the test set of DRIVE database) are slightly skewed. The statistical results are mentioned in Table 4.2. So, we examine all extreme value pdf such as Gumbel, Weibull and Frechet pdfs to design a matched filter kernel for the retinal blood vessels segmentation, because the extreme value pdf curves are slightly skewed. The average accuracy of Gumbel, Weibull and Frechet pdf based matched filter approach for retinal image segmentations are evaluated experimentally and found to be 0.9522, 0.9513, and 0.9509 respectively. On the basis of an experimental result it is found that the Gumbel pdf based matched filter approach achieved better result with respect to the Weibull and Frechet pdf based matched filter approach. Therefore, in this chapter we propose the Gumbel pdf based matched filter approach to achieve better retinal blood vessel segmentation result. The detailed theoretical aspect of above justifications are presented in section 4.3.2 and validated through experimental results shown in results and performance analysis section.

4.3 Methods and model

Our proposed retinal blood vessels extraction approach belongs to the category of matched filter based approach.The block digram of the proposed approach, shown in Figure 4.5,

is the combination of pre-processing, Gumbel pdf based matched filtering, entropy based optimal thresholding, vessel length filtering and removing outliers artifact by using the concept of masking.

4.3.1 Pre-processing

The contrast difference of the retinal blood vessels with respect to their background is low and their contrast decreases, when one move away from the optical disk of the retinal image. Hence, to improve the accuracy of retinal blood vessel segmentation, the contrast enhancement of gray scale retinal image is a prominent pre-processing task. The pre-processing module of proposed approach contains two steps, in first step the RGB color retinal image is converted into gray scale image and in second step the gray scale image is enhanced. To convert the RGB color retinal image into gray scale image various authors [149], [160], [161],[162],[12],[2],[163] used only green channel image of RGB color retinal image for generating the gray scale image, because the contrast of the blood vessels in the green channel image is better in comparison to the red and blue channels of RGB color retinal image. The green channel image is converted into gray scale image by using 'rgb2gray' function available in Matlab (say Method-1) based on weighted sum of the R, G, and B components and then the successive step of particular retinal blood vessel segmentation approaches are applied on gray scale image.

In this approach, Principal Component Analysis (PCA) based color-to-gray image conversion method (say Method-2), is used to generate a gray scale image of color retinal image because, the PCA based color-to-gray conversion method effectively preserves both the texture and color discriminablity by using simple linear computations in subspaces with low computational complexity [164]. The average SNR value has been evaluated by using Eq^n-4.1, to compare the quality of gray scale retinal image generated from Method-1 and Method-2 for all 20 retinal images selected from test set of DRIVE database as given in the Table 4.1. On the basis of average SNR as given in the Table 4.1, it is clear that the quality of gray scale images generated from Method-2 is better with respect to Method-1. Therefore, in first step of the pre-processing module, a PCA based color-to-

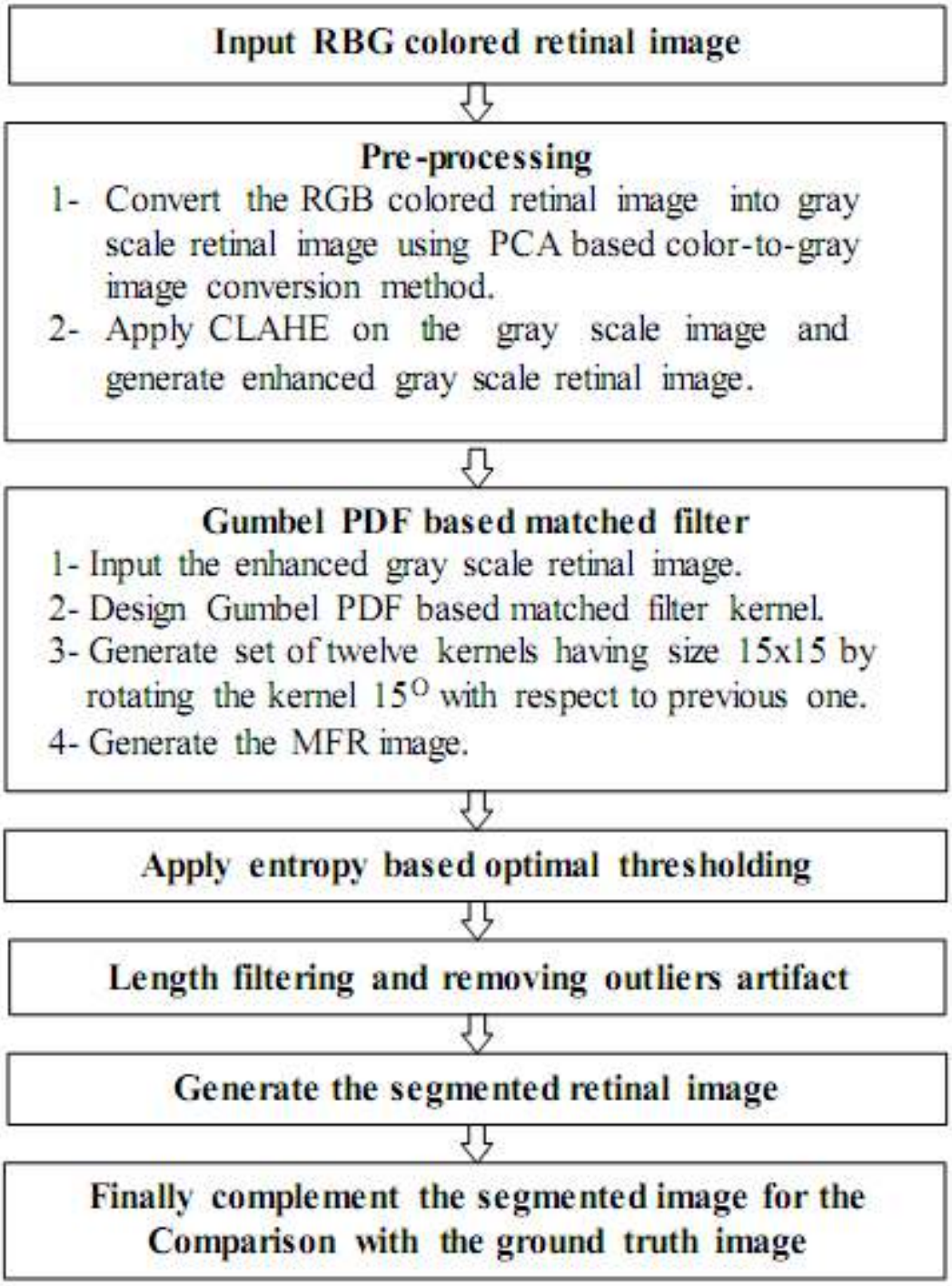

Figure 4.5: Block Diagram of Proposed Approach

gray conversion method (Method-2) is used to generate the gray scale image.

$$Average\ SNR = \frac{Mean\ of\ Image}{Standard\ Deviation\ of\ Image} \tag{4.1}$$

The PCA based color-to-gray conversion method used in pre-processing module con-

tains four steps which are as follows-

- Vectorization of color image by using three color channels (red, green, and blue).
- Finding a zero mean YCbCr image to separate the luminance and chrominance channels.
- Computation of three eigenvalues and respective normalized eigenvectors by using principal component analysis (PCA).
- Application of Eigenvalue-weighted Linear Sum of Subspace Projection (ELSSP) algorithm [164] generate gray scale image. (Figure 4.6(a), (c))

In second step of pre-processing module, a Contrast limited Adaptive Histogram Equalization (CLAHE) method is applied on the gray scale retinal image found in first step of module and the contrast enhanced gray scale image as shown in Figure 4.6(b),(d) is generated. The average SNR value of enhanced gray scale image generated after completing pre-processing module has been evaluated for all 20 retinal image selected from test set of DRIVE database by using Eq^n-4.1 and presented in the Table 4.1. The average SNR of enhanced gray scale image after completing pre-processing module indicates that their quality is improved.

4.3.2 Proposed Gumbel pdf based Matched filter

The matched filter based retinal blood vessel segmentation approach compares the gray scale cross section profile of retinal blood vessels with the predefined kernel. The Chaudhuri *et al.* [12] proposed a first matched filter approach based on Gaussian function and claimed the vessel cross-section profile is in approximate Gaussian shape. The Gaussian function is defined as:-

$$f(x,y) = -e^{(-x^2/2\sigma^2)} \quad for \quad |y| \leq L/2 \tag{4.2}$$

where σ is the variance and L is the length of piece-wise line segment in the kernel. The actual Gaussian curve is shown in Figure 4.4 (a). The author H. Zolfagharnasa *et al.* [14]

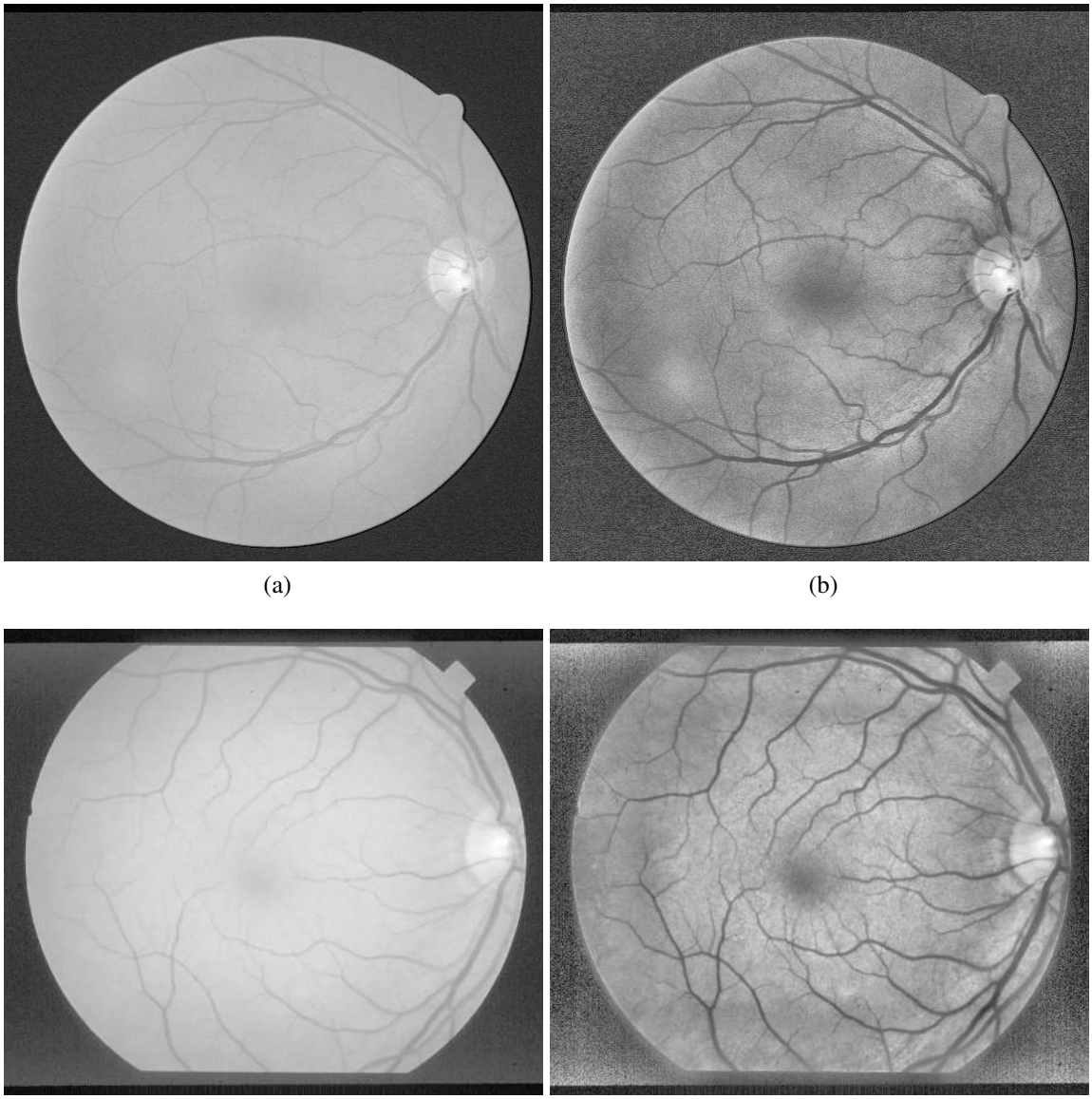

(a) (b)

(c) (d)

Figure 4.6: (a) Gray scale image of '20_test.tif' selected from DRIVE dataset (b) Contrast enhanced gray scale image of '20_test.tif' selected from DRIVE dataset (c) Gray scale image of 'im0082.ppm' selected from STARE dataset (d) Contrast enhanced gray scale image of 'im0082.ppm' selected from STARE dataset

proposed a Cauchy pdf based matched filter approach and claimed the vessel cross-section profile matched better with Cauchy pdf curve as shown in Figure 4.4(b). The Cauchy pdf is defined as:-

$$f(x) = \frac{1}{\pi\gamma\left[1+\left(\frac{(x-x_0)}{\gamma}\right)^2\right]} \tag{4.3}$$

where γ is scale parameter and behaves like a variance used in Eq^n-4.2 and x_0 is location parameter used to shift the peak position of cauchy curve in x-axis. As shown in

Figure 4.4(a) and (b) the Gaussian and Cauchy pdfs both equally diminish towards their truncated values on both sides of their peak value but the Gaussian function reaches to its truncated value faster with respect to the Cauchy pdf.

If we analyse the vessel cross-section intensity profile of the region marked in Figures 4.1(a) and Figures 4.1(b) as shown in Figures 4.2(a) and Figures 4.2(b) by selecting 80 pixels between two points or their well shape cross-section intensity profile as shown in Figures 4.3(a) and Figures 4.3(b), by selecting 30 pixels between two points, then it is clear that the cross-section intensity profile does not equally diminish toward their truncated values on both sides of their peak value and moderately skewed with respect to the Gaussian and cauchy pdf curves.

Therefore, the statistical analysis is required to justify that the gray scale intensity profile curve of retinal image is moderately skewed and not an approximate Gaussian shape. Generally the histogram of image can provide the basic idea about the skewness, but there are some common statistical methods proposed by Cunnane *et al.* [165], Chausse *et al.* [166], Kochanek *et al.* [167] and Joanes and Gill [168] which provide a more precise evaluation to measure the skewness. The skewness is evaluated for gray scale profile data of retinal image by using the statistical method proposed by Joanes and Gill [168]. The moment coefficient of skewness for gray scale data of retinal image is evaluated by using following Eq^n.

$$Skewness(\tau) = M_3 \ / \ M_2^{(3/2)} \tag{4.4}$$

where M_2 and M_3 is second and third moment of gray scale data set and evaluated by using the following $Eq^{n's}$

$$\overline{X} = \sum_{i=1}^{N} X_i \ / \ N \tag{4.5}$$

$$M_2 = \sum_{i=1}^{N} (X_i - \overline{X})^2 \ / \ N \tag{4.6}$$

$$M_3 = \sum_{i=1}^{N} (X_i - \overline{X})^3 \ / \ N \tag{4.7}$$

where $\overline{X}$ is known as mean of the data set and N is number of element in a data set. The median and mode for gray scale data of retinal image is also evaluated. All the statistical

measures for all 20 retinal image taken from test set of DRIVE database are given in the Table 4.2.

After analysis of statistical measures as reported in the Table 4.2, we found two facts that indicate the gray scale cross-section intensity profile of retinal image is not approximate Gaussian shape. First, the mean, median, and mode of all 20 retinal images (as shown in the Table 4.2) are not equal which contradict the Gaussian characteristic (the value of mean, median, and mode must be equal or approximate equal). Second reason is the skewness (τ) that predict, the gray scale cross-section intensity profile of retinal image is not approximate Gaussian shape. According to classical rule of thumb suggested by author Bulmer *et al.* [169] to interpret the skewness, it is observed that the value of skewness of all 20 retinal image taken from test set of DRIVE database belong in between -1 and -0.5. Therefore, the gray scale cross-section profile curve of retinal image is moderately skewed rather than approximate Gaussian. A classical rule of thumb to interpret the skewness given by Bulmer *et al.* [169] are as follows-

$$\begin{cases} \text{Perfectly Skewed,} & \text{if } \tau = 0 \\ \text{Highly skewed,} & \text{if } (\tau < -1) \text{ or } (\tau > 1) \\ \text{Moderately Skewed,} & \text{if } \tau \in (-1, -0.5) \text{ or } (0.5, 1) \\ \text{Approximately symmetric,} & \text{if } \tau \in (-0.5, 0.5) \end{cases}$$

Due to above two reasons, we proposed a novel Gumbel pdf based matched filter approach to segment the retinal blood vessels. The Gumbel pdf is an extreme value probability distribution function having skewed characteristics and defined as:-

$$f(x,y) = \frac{1}{\beta} e^{\frac{X-\mu}{\beta}} e^{-e^{\frac{X-\mu}{\beta}}} \quad for \;\; |y| \leq L/2 \tag{4.8}$$

where X is the perpendicular distance between point (x, y) and straight line passing through the center of retinal blood vessel, μ and β are the location and scale parameter respectively and L is the piece-wise line segment in the kernel.

At first we discuss about scale parameter (β), location parameter (μ) used in Gum-

bel pdf and then discuss about the piece-wise line segment (L) in the kernel. The scale parameter (β) must be a positive real number. The behavior of β used in Gumbel pdf is similar to the variance (σ) and scale parameter (γ) used in Gaussian and Cauchy pdf respectively. For small value of β, the Gumbel pdf curve narrows down and for large value of β, the Gumbel curve expands as shown in Figure 4.4(c). However, the behavior of scale parameter (β) used in Gumbel pdf is different from σ and γ with respect to their diminishing behavior towards their truncated value as previously discussed and clearly visible in Figure 4.4(c).

In addition to the scaling parameter (β), Gumbel pdf has another parameter known as location parameter (μ). The location parameter (μ) shifts the graph on horizontal X-axis. Therefore selection of location parameter (μ) is important. The proposed approach have been tested for some selected values of β (from 0.5 to 3 with 0.5 interval), at different location (μ=0 to 3 with 0.5 interval). After the analysis of obtained results for all 42 different possible combinations of μ and β as shown in Figure 4.7, it is observed that the highest average accuracy of retinal blood vessel segmentation is achieved at μ=1.0 and β=0.5. So in the proposed approach we select 1.0 as the value of location parameter (μ) and 0.5 as the value of scale parameter (β).

According to the Chuadhuri *et al.* [12] notation, the length of retinal blood vessels is assumed as piece-wise line segment (L) in the kernel. The length of piece-wise line segment is determined experimentally by analyzing the blood vessels in both normal and abnormal retinal image. This step reduces the possibility of false vessels detection in non-ideal environment [12]. For the experimental analysis, evaluate the average accuracy of retinal blood vessel segmentation for the different values of L varies from 1 to 15 and it was observed that the average accuracy of retinal blood vessel segmentation is continuously increasing from L=1 to 10 after that it decreases from L=11 to onwards as shown in Figure 4.8. Hence, the value of L=10 is selected as the length of piece-wise line segment in the kernel. On the basis of above selected parameters matched filter kernel is designed. To design a matched filter kernel, we assume that the P_x=[x,y] is a point in the kernel, θ_i is the orientation of the i^{th} kernel matched to the retinal blood vessel at an

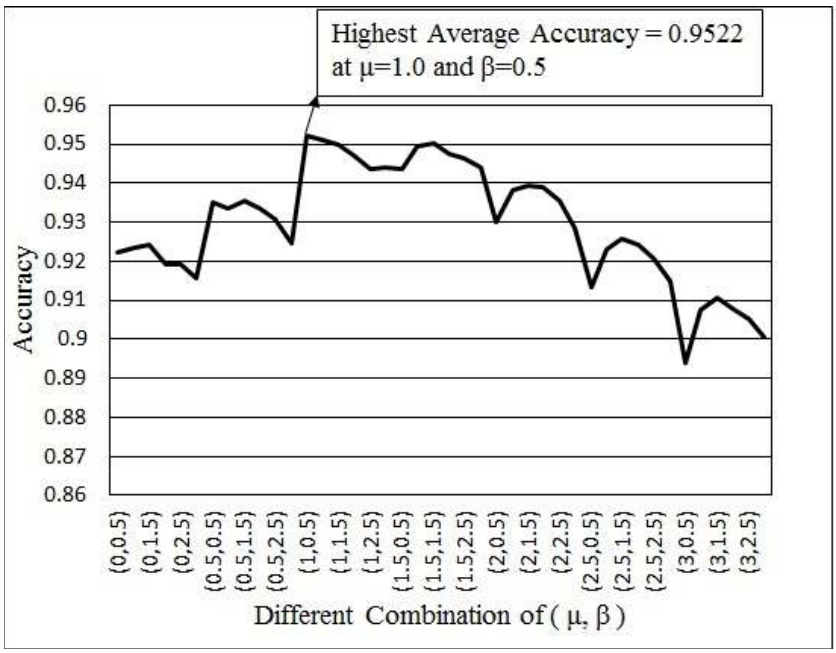

Figure 4.7: Accuracy graph of proposed approach with respect to various combination of μ and β

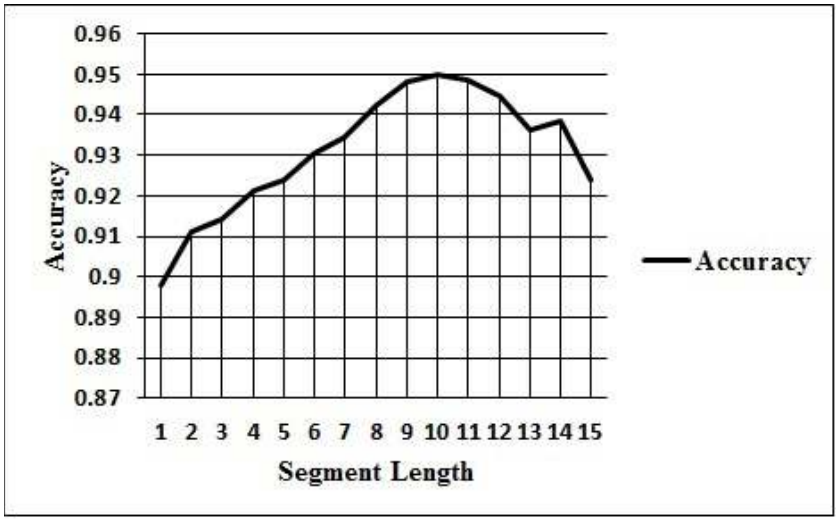

Figure 4.8: Accuracy graph with respect to increasing length of piece-wise line segment

angle θ_i and kernel is centered about the origin. To cover the piece-wise line segments of whole retinal image, a set of twelve kernels having size 15×15 are used in each direction to detect the retinal blood vessels by rotating the kernel 15^o with respect to the previous one. The author Azegrouz *et al.* [146] state that in general the width of retinal blood vessels are 10 pixels but in presence of retinal pathology it may increase upto 3 to 5 pixels depends on the stage of the retinal pathology. Therefore, we select the kernel size 15×15 which is able to segment the healthy as well as pathological retinal image. These twelve

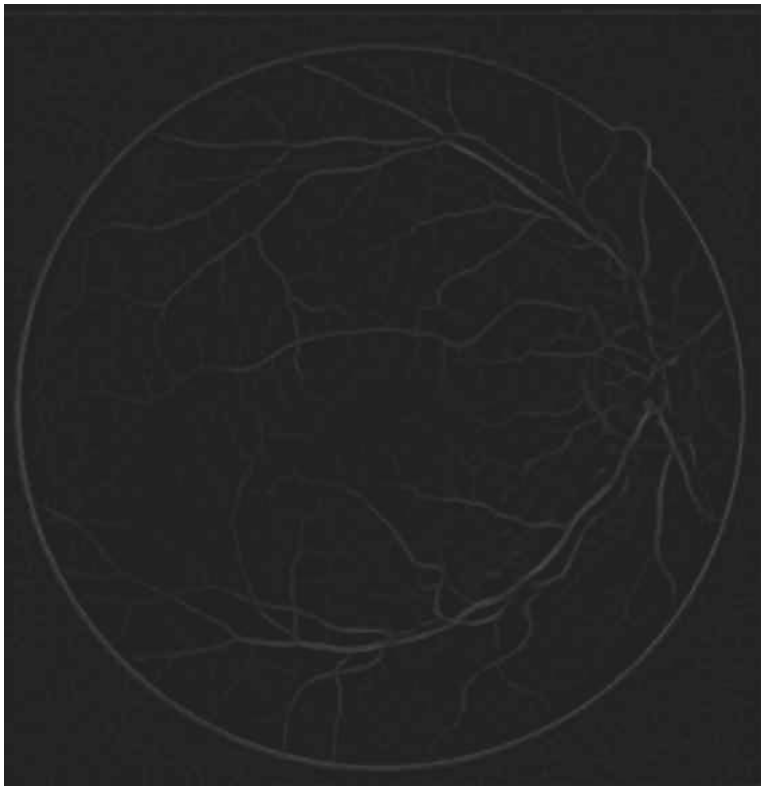

Figure 4.9: MFR image of '20_test.tif' taken from DRIVE data set

kernels with different orientations are calculated by using the following rotation matrix (Rm_i) which is defined as:

$$Rm_i = \begin{bmatrix} Cos\theta_i & -Sin\theta_i \\ Sin\theta_i & Cos\theta_i \end{bmatrix} \tag{4.9}$$

The corresponding point $P_{x_i} = [R_x, R_y]$ in the rotated coordinate system is obtained by

$$P_{x_i} = [R_x, R_y] = P_x \, Rm_i^T \tag{4.10}$$

After constructing twelve different kernels based on Gumbel pdf, it is applied on the gray scale retinal image and then convolved the twelve different kernels and found the matched filter response (MFR) image. The MFR image of retina image '20_test.tif' taken from DRIVE data set is shown in Figure 4.9.

4.3.3 Entropy based optimal thresholding

After applying the proposed matched filtering approach, to produce the binary image of retinal blood vessel structure from the Gumbel pdf based matched filter response (MFR) image, an efficient thresholding algorithm is applied. For this purpose, we use entropy based optimal thresholding algorithm [170],[171] ,[14] was used. The entropy based optimal thresholding algorithm is better than other thresholding algorithms. Reason behind this is that the dependencies between the pixel's intensities of MFR image allows us to preserve the spatial structure of the thresholded images and are able to correctly classify the retinal blood vessels from their backgrounds as argued in [170],[171],[14]. The segmented retinal blood vessels from their background are shown in Figure 4.10(a) and Figure 4.11(a) for image '18_test.tif' and 'im0082.ppm' taken from DRIVE and STARE database respectively.

4.3.4 Length filtering and removing outliers artifact

After observing the Figure 4.10(a) and Figure 4.11(a) generated in previous step, it is found that some isolated and misclassified pixels are still present. To remove these isolated and misclassified pixels, length filtering by using eight-connected neighborhood and pixel label propagation [12] is applied to find a retinal blood vessels structure, as shown in Figure 4.10(b) and Figure 4.11(b). It may be possible that some artifacts outside the region of interest may be included in retinal boundary. Hence, for removing these artifacts the masking is applied by using the mask generated by particular retinal image, as shown in Figure 4.10(c) and Figure 4.11(c). Finally, compliment of the segmented image (shown in Figure 4.10(d) and Figure 4.11(d)) is generated for evaluating the TPR (sensitivity), FPR (1-specificity) and accuracy with respect to ground truth image given in DRIVE and STARE databases respectively.

4.4 Results and discussions

The proposed Gumbel-MF method was implemented on two publicly available retinal image data sets, the DRIVE [137] and the STARE data set[2]. The brief description of these database are presented in Chapter 2, section 2.5. The proposed vessels segmentation approach have been implemented on Matlab R2013a on a PC having AMD E-450 APU, Radeon with 1.65 GHz processor having 2 GB RAM. The average execution time of entire process for 20 images of DRIVE database and 20 images of STARE database took about 2.26 and 2.4 minutes respectively. To compare the performance of the proposed approach, the quantitative performance measures, an average accuracy, Average True Positive Rate (ATPR), and the Average False Positive Rate (AFPR) are calculated. These quantitative performance measures are widely used and defined in literature[2, 44, 12, 26, 27, 66, 48, 56]. The accuracy of the segmentation algorithms is

Table 4.1: SNR of 20 retina image generated from Method-1,2 to justify the pre-processing module of proposed approach

DRIVE Image	**SNR value of Method-1**	**SNR value of Method-2**	**SNR value after Pre-processing**
01_test.tif	1.5654	2.1815	3.1284
02_test.tif	1.5492	2.1411	3.0520
03_test.tif	1.6276	2.3653	3.0479
04_test.tif	1.4961	2.1595	3.0345
05_test.tif	1.5778	2.2201	3.1536
06_test.tif	1.5750	2.1868	3.0149
07_test.tif	1.5115	2.1593	3.0114
08_test.tif	1.5394	2.1783	3.0815
09_test.tif	1.5631	2.1440	3.1299
10_test.tif	1.5563	2.2408	3.2033
11_test.tif	1.5127	2.1425	3.0430
12_test.tif	1.5665	2.1811	3.1422
13_test.tif	1.5409	2.1417	3.0676
14_test.tif	1.5757	2.2254	3.1923
15_test.tif	1.4596	2.2248	3.1677
16_test.tif	1.5610	2.1490	3.0307
17_test.tif	1.5635	2.1287	2.9782
18_test.tif	1.5528	2.1338	3.0628
19_test.tif	1.5810	2.2634	3.0666
20_test.tif	1.5713	2.1931	3.1826

Table 4.2: Various Statistical Measures to justify the skewness of 20 retina image

Image	**Mean**	**Median**	**Mode**	M_2	M_3	**Skewness** (τ)
01_test.tif	148.06	188	267.89	4604.35	-242695.15	-0.7768
02_test.tif	152.1	194	277.8	5045.31	-278036.39	-0.7758
03_test.tif	156.46	195	272.07	4377.06	-226776.03	-0.7831
04_test.tif	141.29	176	245.42	4279.76	-193265.75	-0.6903
05_test.tif	145	184	262	4263.94	-218551.82	-0.7849
06_test.tif	149.98	191	273.03	4699.75	-251779.28	-0.7815
07_test.tif	148.5	188	266.99	4727.6	-232268.03	-0.7145
08_test.tif	141.3	179	254.4	4203.16	-203531.93	-0.7469
09_test.tif	151.09	194	279.81	4964.39	-276562.93	-0.7907
10_test.tif	140.46	174	241.09	3925.92	-184035.75	-0.7482
11_test.tif	148.16	185	258.67	4781.76	-240843.69	-0.7284
12_test.tif	146.99	187	267.02	4538.55	-240859.49	-0.7878
13_test.tif	147.22	188	269.55	4721.27	-246964.19	-0.7613
14_test.tif	151.06	191	270.87	4608.04	-245531.04	-0.7849
15_test.tif	132.39	160	215.22	3538.84	-126247.33	-0.5997
16_test.tif	152.11	195	280.78	5007.34	-279220.74	-0.7880
17_test.tif	155.18	200	289.64	5311.74	-307255.38	-0.7937
18_test.tif	151.36	194	279.29	5029.22	-279546.3	-0.7838
19_test.tif	141.36	177	248.29	3896.11	-185926.39	-0.7645
0_test.tif	139.85	178	254.31	4063.98	-202583.73	-0.7819

defined as the ratio of total correctly classified pixels with total number of pixels in the selected image. The TPR is the ratio of total correctly classified vessel pixels with total number of vessel pixels in the respective ground truth image and similarly the FPR is the ratio of total correctly classified non-vessel pixels with total number of non-vessel pixels in the respective ground truth image. The brief description of performance measures are presented in Chapter 2, section 2.4.1. The values of these performance measures are shown in Table 4.3 and Table 4.5 for DRIVE and STARE database respectively.

The proposed approach is compared with three prominent matched filter approaches, namely a classical Gaussian matched filter approach introduced by author Chaudhuri *et al.* [12], improved matched filter approach introduced by Al-Rawi *et al.* [13], and Cauchy matched filter approach introduced by H. Zolfagharnasab *et al.* [14] as well as some other segmentation approaches proposed by Zhang *et al.* [47], Xiaoyi *et al.* [44], Cinsdikici *et al.* [45], Amin *et al.* [46], D Marin *et al.* [53], and Lam *et al.* [157]. All 20 retinal images of test set from DRIVE data set are used for comparative analysis. The ATPR, AFPR,

Table 4.3: Quantitative performance measures of 20 images taken from DRIVE database

DRIVE Image	**TPR**	**FPR**	**Accuracy**
01_test.tif	0.8613	0.0433	0.9482
02_test.tif	0.7372	0.0168	0.9580
03_test.tif	0.7673	0.0465	0.9350
04_test.tif	0.7441	0.0221	0.9564
05_test.tif	0.7860	0.0325	0.9505
06_test.tif	0.6726	0.0187	0.9512
07_test.tif	0.7488	0.0370	0.9435
08_test.tif	0.6745	0.0245	0.9496
09_test.tif	0.6961	0.0188	0.9581
10_test.tif	0.7218	0.0261	0.9531
11_test.tif	0.7630	0.0416	0.9409
12_test.tif	0.7678	0.0283	0.9541
13_test.tif	0.7058	0.0258	0.9480
14_test.tif	0.8023	0.0348	0.9520
15_test.tif	0.7954	0.0390	0.9492
16_test.tif	0.7588	0.0209	0.9592
17_test.tif	0.6917	0.0201	0.9555
18_test.tif	0.8168	0.0283	0.9594
19_test.tif	0.8586	0.0338	0.9573
20_test.tif	0.8183	0.0248	0.9637
Average	**0.7594**	**0.0292**	**0.9522**

Table 4.4: Comparative Analysis of proposed approach for DRIVE database

Segmentation Approach	**ATPR**	**AFPR**	**Average accuracy**	**AUC**
Classical Gaussian MF [12]	0.6326	0.0936	0.8709	0.7878
Improved Gaussian MF [13]	0.5993	0.0447	0.9096	0.9435
Cauchy MF [14]	0.6239	0.0286	0.9269	—
Zhang *et al.* [47]	0.7120	0.0276	0.9382	—
Xiaoyi *et al.* [44]	—	—	0.9212	0.9114
Cinsdikici *et al.* [45]	—	—	0.9293	0.9407
Amin *et al.* [46]	—	—	0.9200	0.9400
Marin *et al.* [53]	0.7067	0.0199	0.9452	0.9588
Lam *et al.* [157]	—	—	0.9472	0.9614
Proposed approach	**0.7594**	**0.0292**	**0.9522**	**0.9287**

and average accuracy of proposed approach and previously mentioned approaches are reported in Table4.4. According to results analysis, the performance measures of proposed approach is found better in comparison to the prominent matched filter approaches as well as other matched filter based approaches. The average accuracy of proposed approach is better by 8.13%, 4.26%, 2.53%, 1.42%, 3.10%, 2.29%, 3.22%, 0.70%, and 0.50% with

Table 4.5: Quantitative performance measures of 20 images taken from STARE database

STARE Image	**TPR**	**FPR**	**Accuracy**
im0001.ppm	0.7299	0.0995	0.8869
im0002.ppm	0.7993	0.0990	0.8942
im0003.ppm	0.7537	0.1008	0.8905
im0004.ppm	0.4917	0.0238	0.9403
im0005.ppm	0.8383	0.0929	0.9009
im0044.ppm	0.9001	0.1017	0.8984
im0077.ppm	0.8397	0.0707	0.9222
im0081.ppm	0.8806	0.0708	0.9255
im0082.ppm	0.8518	0.0565	0.9363
im0139.ppm	0.8087	0.0611	0.9284
im0162.ppm	0.8094	0.0448	0.9448
im0163.ppm	0.8427	0.0301	0.9600
im0235.ppm	0.8298	0.0495	0.9398
im0236.ppm	0.8298	0.0508	0.9384
im0239.ppm	0.7732	0.0357	0.9478
im0240.ppm	0.8114	0.0983	0.8925
im0255.ppm	0.7891	0.0365	0.9479
im0291.ppm	0.8291	0.0542	0.9399
im0319.ppm	0.7019	0.0248	0.9634
im0324.ppm	0.7679	0.0462	0.9414
Average	**0.7939**	**0.0624**	**0.9270**

Table 4.6: Comparative Analysis of proposed approach for STARE Database

Segmentation Approach	**ATPR**	**AFPR**	**Average accuracy**	**AUC**
Hoover *et al.* [2]	0.6751	0.0433	0.9267	—
Kande[54]	—	—	0.8976	0.9298
Cauchy MF [14]	0.6239	0.0286	0.9269	—
Zhang *et al.* [61]	0.7373	0.0264	0.9087	—
Perez *et al.* [67]	0.7790	0.0591	0.9240	—
Palomera *et al.* [64]	0.7690	0.0551	0.9260	—
Xiaoyi *et al.* [44]	—	—	0.9009	0.8906
Proposed approach	**0.7939**	**0.0624**	**0.9270**	**0.9140**

respect to average accuracy of approaches introduced by Chaudhuri *et al.* [12], Al-Rawi *et al.* [13], H. Zolfagharnasab *et al.* [14] , Zhang *et al.* [47], Xiaoyi *et al.* [44], Cinsdikici *et al.* [45], Amin *et al.* [46], D Marin *et al.* [53], and Lam *et al.* [157] respectively. After that for all 20 retinal images of STARE data set, we compared the ATPR, AFPR, and average accuracy of proposed approach with other approaches introduced by Hoover *et al.* [2], Kande[54], Zhang *et al.* [61], Perez *et al.* [67], Palomera *et al.* [64] and Xiaoyi

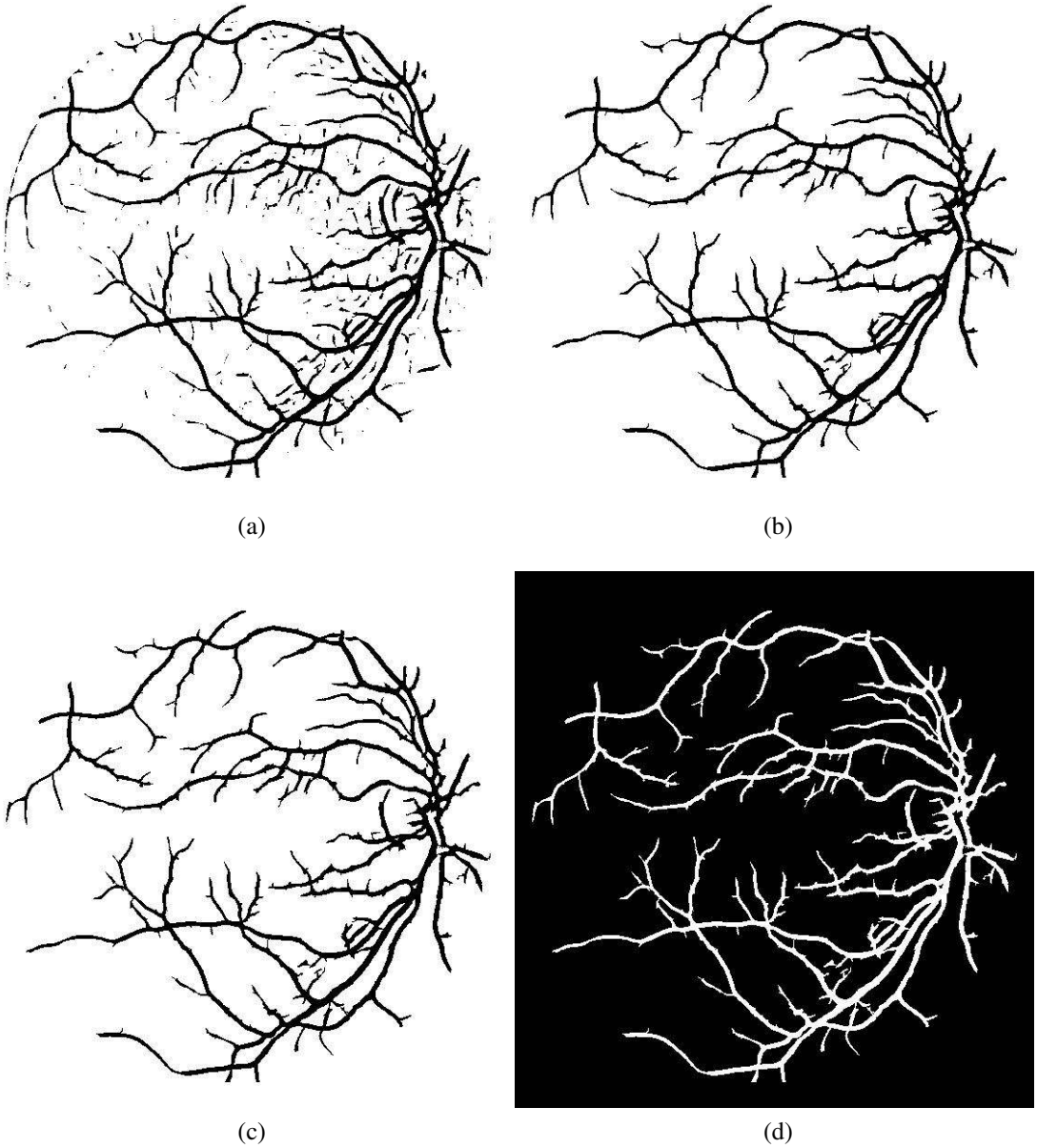

(a) (b)

(c) (d)

Figure 4.10: Details of image '18_test.tif' taken from DRIVE data set (a) classified blood vessels from their backgrounds (b) blood vessel without isolated and misclassified pixels (c) after removing outliers artifact (d) complimented segmented image for comparison with the existing Ground Truth Image

et al. [44]. According to the comparative analysis as reported in Table 4.6, it is found that the average accuracy of proposed approach is better by 0.03%, 2.94%, 1.83%, 0.30%, 0.10%, and 2.61% with respect to average accuracy of approaches introduced by Hoover *et al.* [2], Kande[54], Zhang *et al.* [61], Perez *et al.* [67], Palomera *et al.* [64], and Xiaoyi *et al.* [44] respectively.

Other than the quantitative performance measures, the receiver operating characteris-

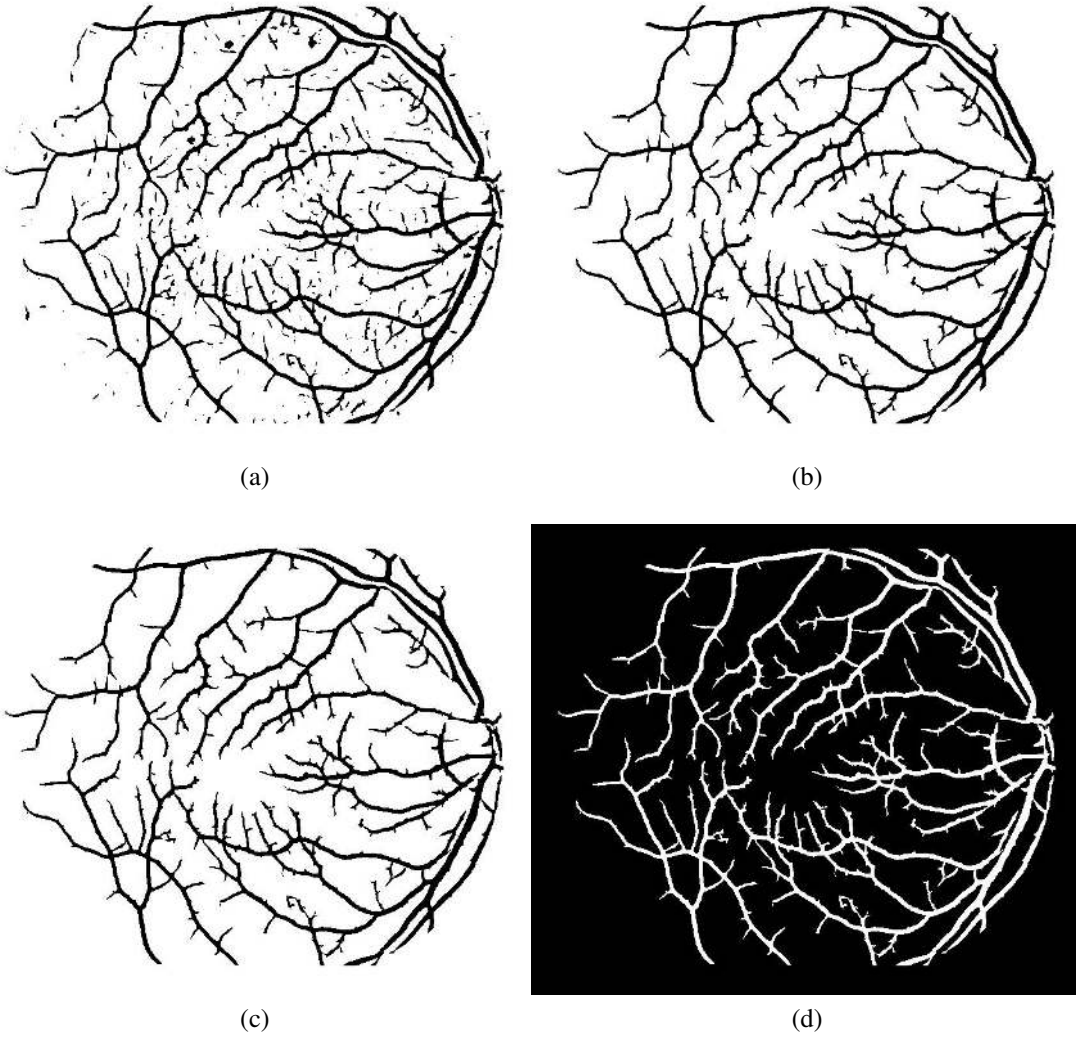

(a) (b)

(c) (d)

Figure 4.11: Details of image 'im0082.ppm' taken from STARE data set (a) classified blood vessels from their backgrounds (b) blood vessel without isolated and misclassified pixels (c) after removing outliers artifact (d) complimented segmented image for comparison with the existing Ground Truth Image

tic (ROC) curve is used to justify the effectiveness of the segmentation approach [172]. ROC curve is a graphical representation of TPR on the y-axis and FPR on x-axis. The area under the curve (AUC) is an important component of ROC for justify the effectiveness of any segmentation approach. The maximum value of AUC is 1 which indicates segmentation approach is perfect for differentiating the true vessels from their background that means the number of false positive and false negative pixels must be zero, which is practically not possible [172]. If the value of AUC closer to 1 which indicates the better performance of the segmentation approach [172].

Therefore, to justify the effectiveness of proposed approach, we plot the ROC curve

and calculate the AUC by using the ATPR and AFPR for both the DRIVE and STARE data set as shown in Figure 4.12 and Figure 4.13 respectively. The value of average AUC is 0.9287 and 0.9140 for the 20 retinal images of DRIVE and STARE data sets respectively. In both cases, value of AUC is closer to 1 which indicates that the performance of proposed Gumbel pdf based matched filter approach for retinal blood vessels segmentation is better.

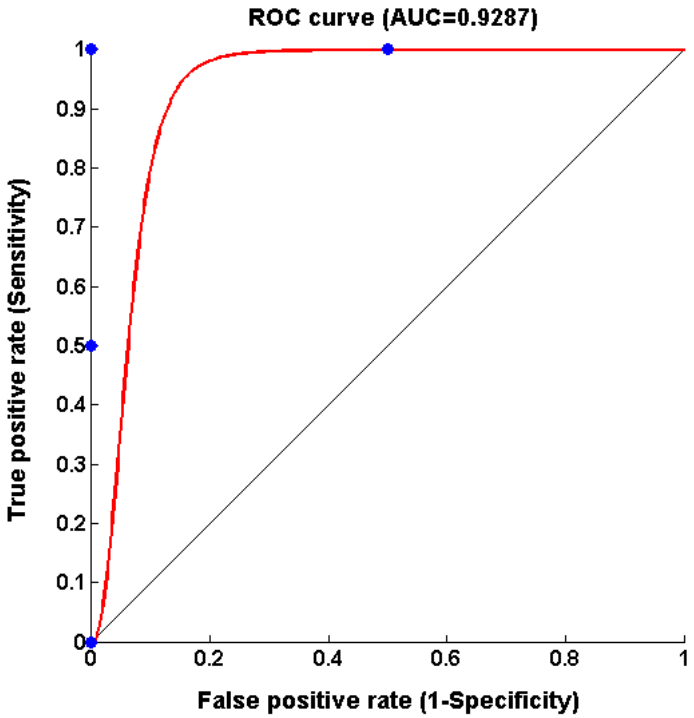

Figure 4.12: ROC Curve for DRIVE data set

4.5 Conclusion

The retinal blood vessels are responsible for the detection of retinal pathology therefore segmentation of retinal blood vessels from their background is a prominent task. In this chapter, we presented a novel matched filter approach with the Gumbel probability distribution function as its kernel. In the proposed approach, a customary Gaussian function used by prominent researchers [12], [13] and Cauchy probability distribution function used by [14] was replaced by Gumbel probability distribution function and achieved the higher accuracy in retinal blood vessel segmentation. The reason to achieve the higher ac-

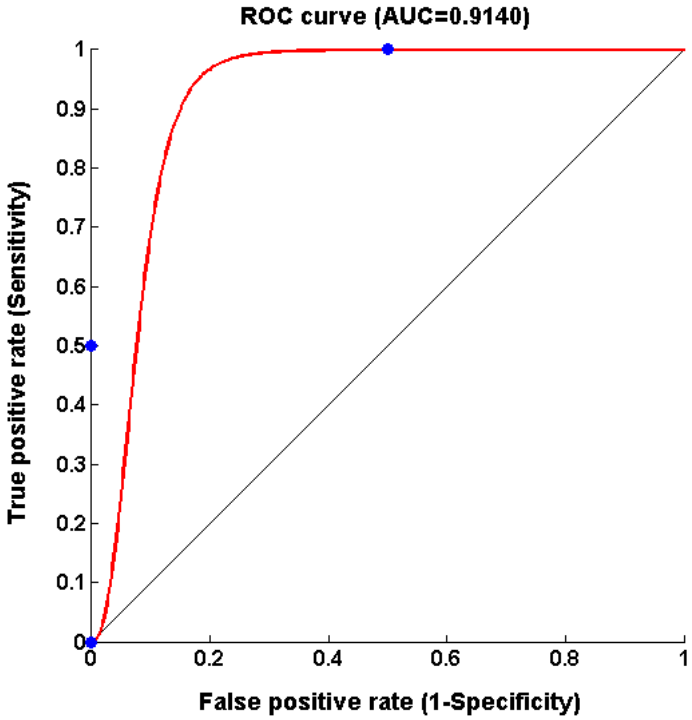

Figure 4.13: ROC Curve for STARE data set

curacy is due to better matching of gray scale cross-sectional profile of retinal image and Gumbel pdf based kernel. The proposed matched filter with the Gumbel pdf as its kernel is compared with respect to the prominent Gaussian distribution function and Cauchy pdf based matched filter approaches and achieved the better performance. For the comparative analysis 20 retinal images have been selected form the test set of DRIVE data set and STARE data set.